Journal of Structural Geology, Vol. 5, No. 1, pp. 47 to 52, 1983
Printed in Great Britain

0191-8141/83/010047-06 $03.00/0

Stress and displacement distributions around pyrite grains

STEFAN O. SELKMAN

Boliden Mineral AB, Saxbergsgruvan, S-772 00 Grängesberg 4, Sweden

(*Received* 1 *February* 1982; *accepted in revised form* 22 *October* 1982)

Abstract—Photomicrographs from two sulfide-mineralized areas in Scandinavia show fragments of pyrite in a relatively homogeneous ground mass. At the extremities of the fragments, quartz segregations are common.

In order to understand the stress and displacement in the development of these mineral segregations, the finite element method has been used. Models have been constructed in order to simulate angular fragments or crystals in an incompetent ground mass, which have been subjected to a differential pressure. Several models have been deformed iteratively, simulating viscous behaviour.

The results indicate that the magnitude of deformation depends on the viscosity contrast, the magnitude of external pressure and the orientation of the inclusion. The stress distribution is governed by the viscosity contrast and the form of the inclusion. The tensile stress areas in the models are comparable to the areas of mineral segregation in the samples.

INTRODUCTION

A STRIKING phenomenon in sulfide-mineralized areas is that pyrite, when present in minor proportions, is sometimes seen to have a preferred orientation. The pyrite grains are often connected to quartz segregations, the orientation of which might reflect how the local stresses in the surrounding rock were built up during the history of deformation. The aim of the present work was to simulate the conditions necessary for the development of these micro-structures, found in highly deformed sulfide mineralized areas, with the emphasis on the deformation history and stress distribution.

The relationships of the mineralogy and structures around fragments, and the magnitude and directions of external pressure (i.e. 'pressure shadow' relationships), have been studied by Pabst (1931), Frankel (1957), Ramberg & Ekström (1964), Durney & Ramsay (1973), Schoneveld (1977) and Ferguson *et al.* (1980). Studies on preferred orientation were made by Kamb (1959), Means & Paterson (1966), Baker *et al.* (1969), Graf & Skinner (1970) and Boer (1977). The strain distributions in experimental models of similar structures which were subjected to external pressure, have been studied by Ghosh & Ramberg (1976), who used modelling clay and painter's putty, and Strömgård (1973), who used photoelastic materials.

In a finite-element study, Selkman (1978), investigated the mineral and stress distribution around boudins. In the present study the same finite-element method has been used. The conditions are now more varied with respect to pressure and structural relations.

SAMPLES USED

Photomicrographs were made of structures from the Långsele sulfide ore and from Storlien in the Caledonides of Sweden. The latter sample was donated by Professor Ramberg of Uppsala.

The mineralization at Långsele consists of massive, pyrite-ore lenses surrounded by sericite–quartzite and volcanic rocks. In these ores, euhedral pyrite grains with elongate, quartz segregations on two mutually opposite sides, are fairly common (Fig. 1). Quartz is commonly replaced by galena, sphalerite and/or pyrrhotite. The highest temperature in the area has been estimated to be about 310°C (Berglund & Ekström 1974).

In the sample from Storlien, elongate pyrite crystals can be seen in an amphibolitic matrix. At the extremities of the crystals, quartz segregations of varying forms are common. When quartz is in direct contact with pyrite, the form of quartz can be seen as a continuation of the elongation. When quartz is not in direct contact with pyrite, it is typically pear-shaped (Fig. 2).

FINITE-ELEMENT MODELS

The finite-element method (FEM) was originally used to estimate the strength of technical constructions

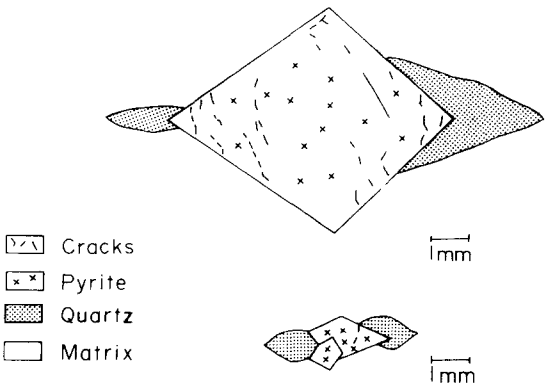

Fig. 1. Pyrite crystals from the Långsele sulfide deposit. Dotted areas are cavities filled with quartz

(Argyris 1955). It is also suitable for solving problems in rock mechanics (Wilson 1963). A brief outline of the finite-element method, its application in rock mechanics and its further use in tectonic studies, is given by Stephansson & Berner (1971). A continuum is replaced by a finite number of elements interconnected at a finite number of nodal points. The method can be used to determine the displacements of the nodal points and the stresses within the elements developed in two- or three-dimensional models with Hookean elastic or Newtonian viscous behaviour. Forces acting on the actual structure are replaced by statically equivalent forces, acting at the nodal points of the finite-element system.

In this investigation, the finite-element method is used to determine the stresses and rates of displacements developed in two-dimensional viscous structures of defined geometry and with constituent materials of different properties. Plane strain is assumed. The basic theory, as developed by Zienkiewicz & Cheung (1967), permits analyses of 'instantaneous' finite displacements and stress distributions of structures in elastic materials. However, if strains are replaced by strain rates and displacements by velocities, the slow motion of linear viscous (Newtonian) materials can be studied.

The basic model in the present investigation consists of a rectangle divided into a large number of square elements (Fig. 3). Each nodal point, at the corners of the elements, has been given coordinates in a two-dimensional, right-angled coordinate system. Each element has been given values for the viscosity, density and Poisson's ratio. The model is deformed under directed pressure at a constant value of the gravity acceleration (9.81 m s^{-2}) and a chosen confining pressure.

Particular models have been constructed to simulate angular fragments or crystals in an incompetent ground mass which has been subjected to a differential pressure.

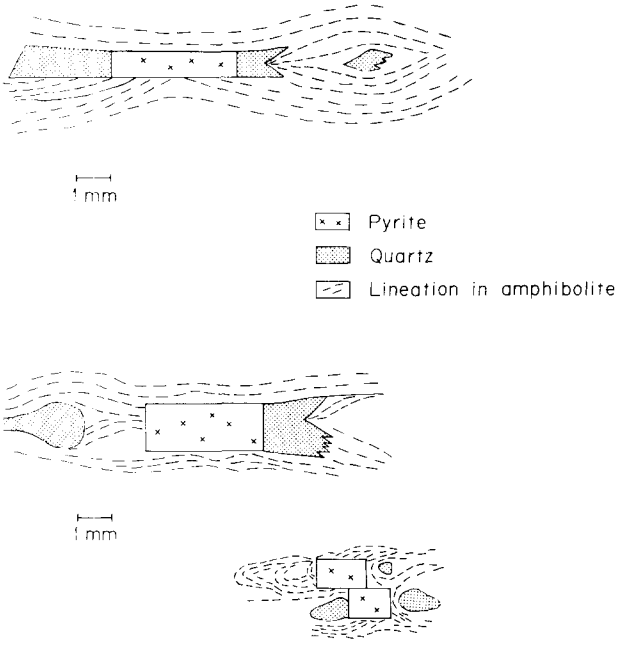

Fig. 2. Parallel and extended pyrite crystals from Storlien in the Swedish Caledonides.

The size of these models has been based on the size of the structures seen in the different sulfide mineralizations (Figs. 1 and 2). Each model measures 4 × 7 cm and consists of about 400 elements.

Three different types of models have been used (Fig. 3), all of which contain an angular inclusion with higher viscosity than its surroundings. The models differ in the position of the inclusion in the coordinate system (X, Y). The deformation takes place parallel to the Y-direction. All models have been given conditions that permit them

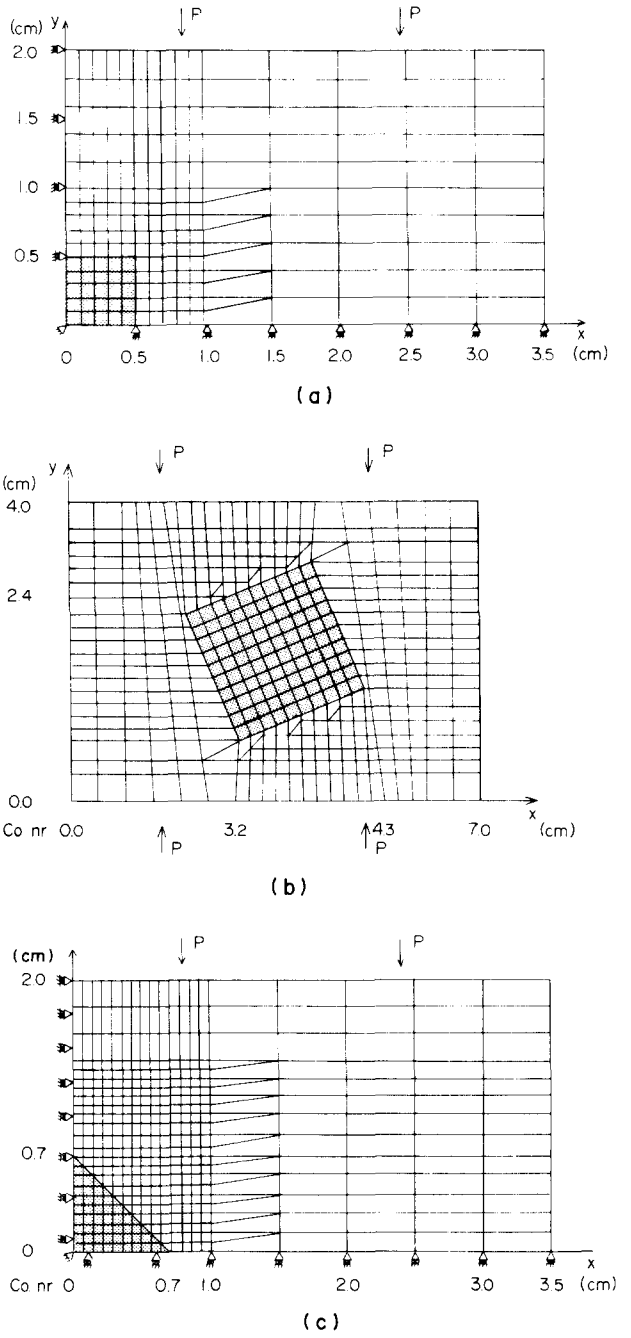

Fig. 3. (a) Model 1, contains a 'competent' viscous object in a less viscous matrix. By symmetry, a quarter of the structure is used. The model is deformed by compression P, perpendicular to the model boundaries (parallel to Y). (b) Model 2, contains a competent object rotated through 22.5° in relation to model 1 but in the same matrix. Similar compression has been applied. (c) Model 3, contains the same competent object as the former models but rotated through another 22.5° in relation to model 2.

to expand freely or against a certain pressure parallel to the X-direction. In most models, the viscosity ratio varies between 9 and 90. The value of Poisson's ratio is 0.45 for all models, while the densities are varied according to the observed natural reference structures.

Owing to the small size of the structures, both the gravity and the density contrast have only marginal effect on the result. Several models have been deformed step-by-step iteratively, which is essential for the evaluation of the deformation. A single step means compression during a certain time. In this way, the models have been compressed up to 8.33% parallel to the directed pressure.

The result is recorded as a displacement of each nodal point and as a stress difference between different elements. Values have been given for both principal stress and shear.

DEFORMATION

The deformation of the models is recorded as a displacement of the nodal points. To illustrate this, lines were drawn through all nodal points with identical displacements (Fig. 4). Examination of these lines shows the following facts.

(1) The matrix is more intensively deformed than the inclusion.
(2) The magnitude of the deformation depends on the viscosity ratio.
(3) The orientation of the inclusion affects the direction and the magnitude of the deformation.
(4) The magnitude of the deformation depends on the magnitude of the external pressure.
(5) The direction of 'flow' tends to become largest perpendicular to the external pressure (Fig. 5).

STRESS DISTRIBUTION

Compression leads to a stress distribution within the model in which the major part of the stress is compressive and the minor part tensile (Figs. 6–8). The compressive stress is parallel or nearly parallel to the external-pressure direction.

The stress distribution is governed by the viscosity ratio and by the form of the inclusion. Although the tensile stress is small, it is considered of decisive importance for the localization of sulfides (Selkman 1978). The sizes of the areas of tensile stress positively correlate with the size of the external pressure; they are also related to the position of the inclusion in the coordinate system. The form of the areas depends on the form and the position of the inclusion and also on the external pressure.

The distribution of shear also depends on the position of the inclusion and on the size of the external pressure (Fig. 9).

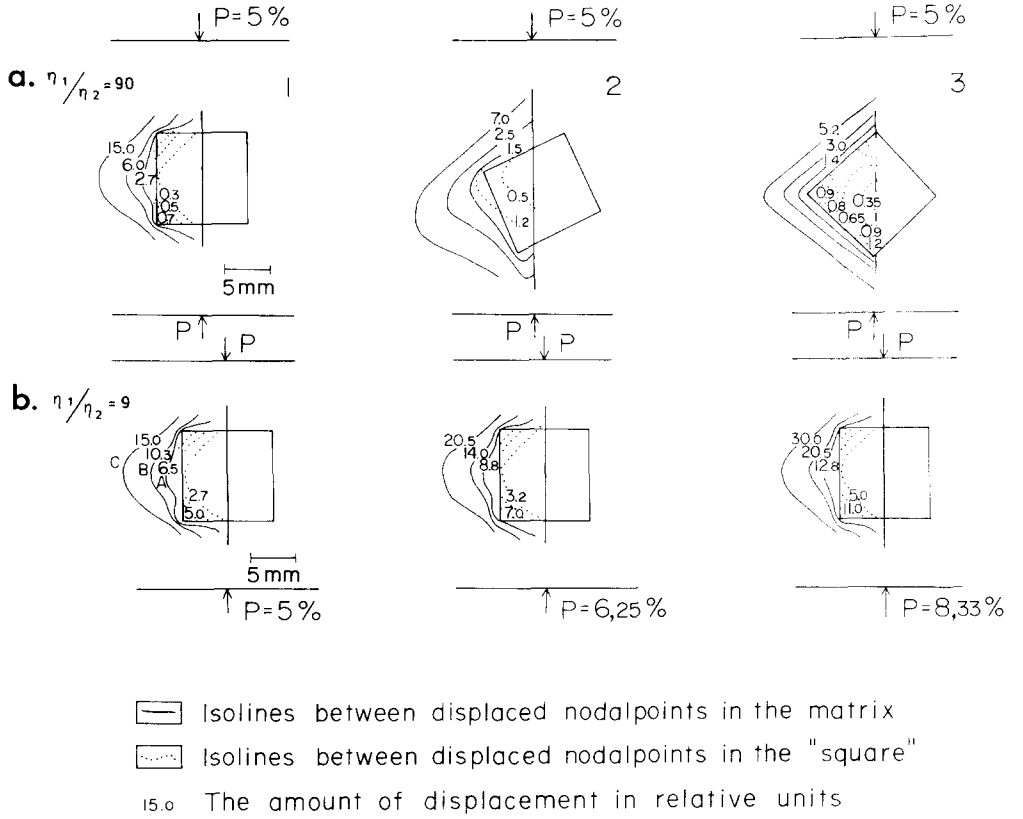

Fig. 4. Displacement of nodal points, combined to form isolines (contours). (a) Models 1, 2 and 3, compressed and shortened by 5%, at a constant value of viscosity ratio = 90. (b) Model 1, compressed and shortened gradually up to 8.3%, at a constant value of viscosity ratio = 9.

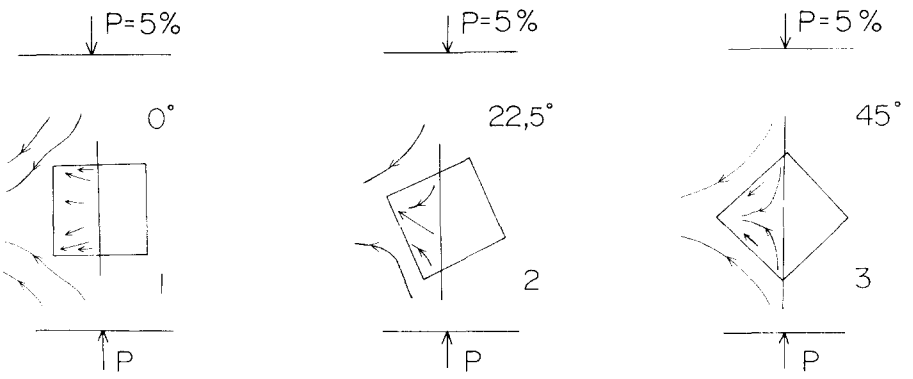

Fig. 5. Flow directions in models 1, 2 and 3 at 5% shortening, constructed from displacement gradients.

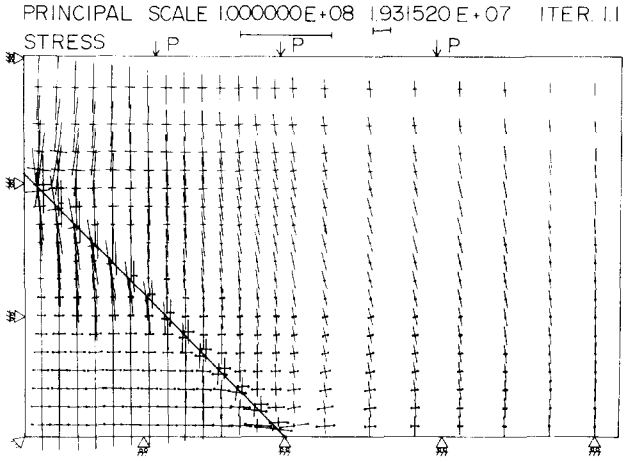

Fig. 6. Distribution of principal stress in model 3. The magnitude of the stress is proportional to the length of the lines. Tensile stress is given by dots.

DISCUSSION

In the selected sample from Långsele, the temperature reached about 310°C and in Storlien, the temperature once reached over 500°C. Heated minerals and mineral assemblages might be expected to behave as Newtonian viscous fluids, the value of viscosity depending on the temperature. The viscosity values of the samples are unknown, but in the FE models, values are varied in order to reflect the behaviour of rocks at different temperature. It is suggested that the models could reflect the stresses and displacements which existed in the two samples.

Flow directions, indicated by displacement gradients in the FE-models of Fig. 5, may be compared to the defined lineation in the matrix of the sample from Storlien (Fig. 2). The boundaries of tensile stress areas in the FE-models vary according to the applied pressure (Fig. 7), the viscosity ratio (Figs. 7 and 8) and the angle of the inclusion edge (Fig. 8). The Storlien sample compares well with model 1 (Fig. 3a) compressed up to 10%. The Långsele sample may be compared with model 3 (Fig. 3c) with a low viscosity ratio.

As the principal tensile stress increases with increasing applied pressure (Fig. 7), and displacement differences increase with increasing viscosity ratios (Fig. 4), within tensile stress areas cracks may form. Cracks should form more easily in the Storlien sample than in the Långsele sample at the same confining pressure. It would be expected that mobile materials from the matrix should be localized in areas of tensile stress and that the velocity of mobilization would depend on the viscosity ratio.

Acknowledgements—Samples were obtained from Boliden Mineral AB and from Professor H. Ramberg. The experiments were performed with digital simulations of models, designed at the Institute of Geology, Department of Mineralogy and Petrology, University of Uppsala, Sweden. The author wishes to thank Professor H. Ramberg for critically reading the manuscript, Professor O. Stephansson and Dr H. Berner for writing the digital program, and Barbro Persson and Margareta Andersson for drawing the figures. Special thanks are due to Dr Örjan Amcoff for being helpful with the translation of the manuscript into English.

REFERENCES

Argyris, J. H. 1955. Energy theorems and structural analyses. *Aircraft Engng* **27**, 42–58, 80–94, 124–134 and 145–158.

Baker, D. W., Wenk, H. R. & Christie, J. H. 1969. X-ray analyses of preferred orientation in fine-grained quartz aggregates. *J. Geol.* **77**, 144–172.

Berglund, S. & Ekström, T. K. 1974. Sphalerite composition in relation to the stress distribution of a boudinage. *Lithos* **7**, 1–6.

Boer, R. B. 1977. Pressure solution: theory and experiment. *Tectonophysics* **39**, 287–301.

Durney, D. W. & Ramsay, J. G. 1973. Incremental strains measured by syntectonic crystal growth. In: *Gravity and Tectonics* (edited by de Jong, K. A. & Scholten, R). Wiley, New York, 67–96.

Ferguson, C. C., Harvey, P. K. & Lloyd, G. E. 1980. On the mechanical interaction between a growing porphyroblast and its surrounding matrix. *Contr. Mineral Petrol.* **75**, 339–352.

Frankel, J. J. 1957. Abraded pyrite crystals from the Witwatersrand gold mines. *Mineralog. Mag.* **31**, 392–401.

Ghosh, S. K. & Ramberg, H. 1976. Reorientation of inclusions by combination of pure shear and simple shear. *Tectonophysics* **34**, 1–70.

Graf, J. L., Jr. & Skinner, B. J. 1970. Strength and deformation of pyrite and pyrrhotite. *Econ. Geol.* **65**, 206–215.

Kamb, N. B. 1959. Theory of preferred orientation developed by crystallization under stress. *J. Geol.* **67**, 153–170.

Means, W. D. & Paterson, M. S. 1966. Experiments on preferred orientation of platy minerals. *Contr. Mineral. Petrol.* **13**, 108–133.

Pabst, A. 1931. 'Pressure shadow' and measurement of orientation of minerals in rocks. *Am. Miner.* **16**, 55–70.

Ramberg, H. & Ekström, T. 1964. Note on preferred orientation of pyrite cubes in grit layers in slate. *Neues Jb. Miner. Mh.* **8**, 246–251.

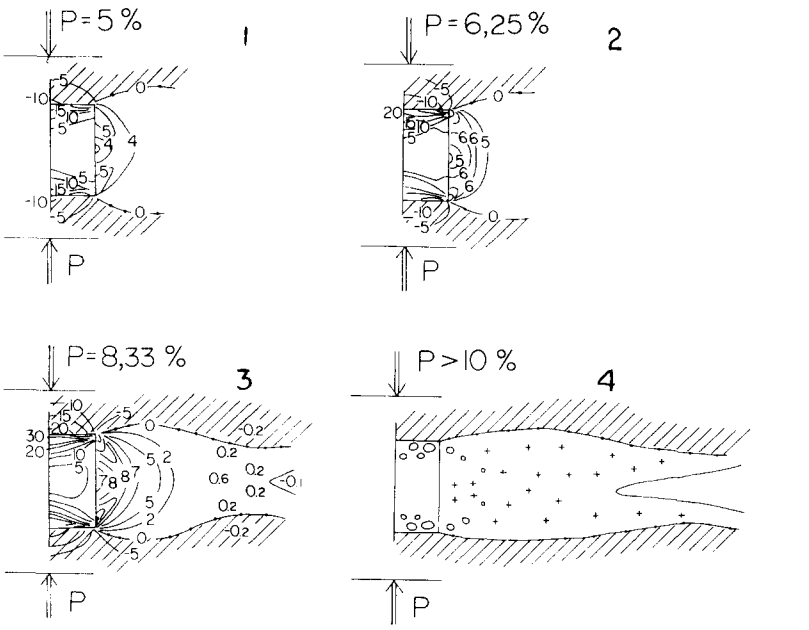

Fig. 7. Distribution of principal tensile stress for model 1 and viscosity ratio 9. Places with large values of tensile stress are concentrated in areas close to the viscosity-contrast boundary.

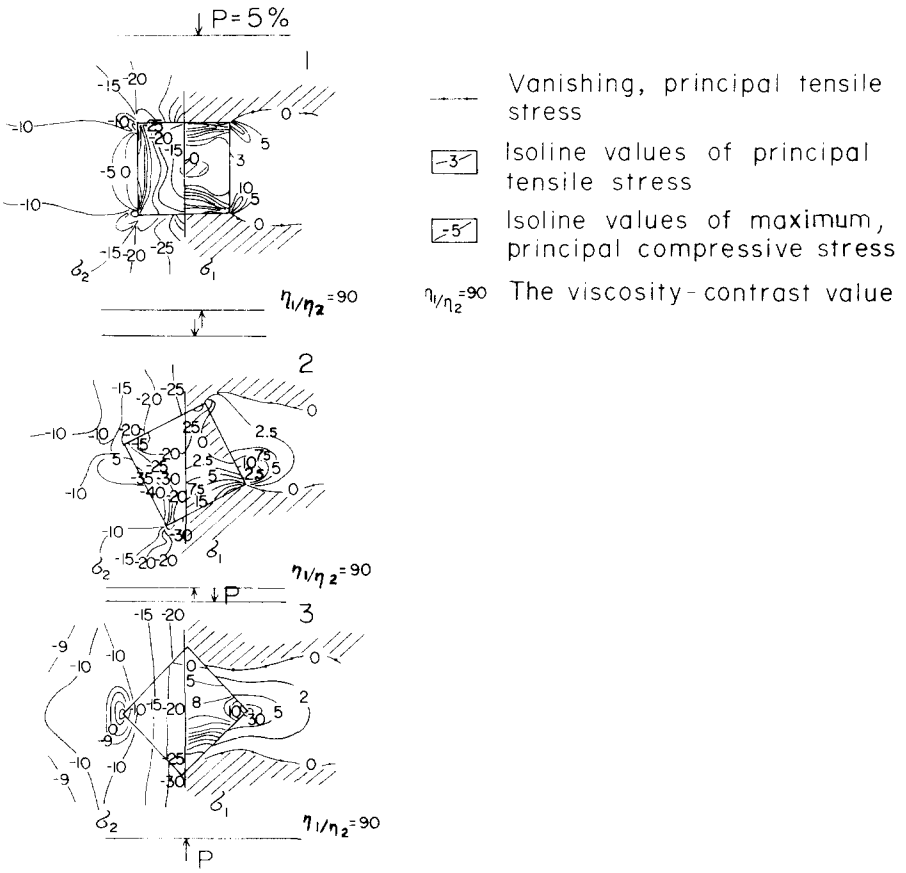

Fig. 8. Principal stress isolines (contours) of models 1, 2 and 3. The left side contains the maximum principal compressive stress and the right side the minimum principal stress.

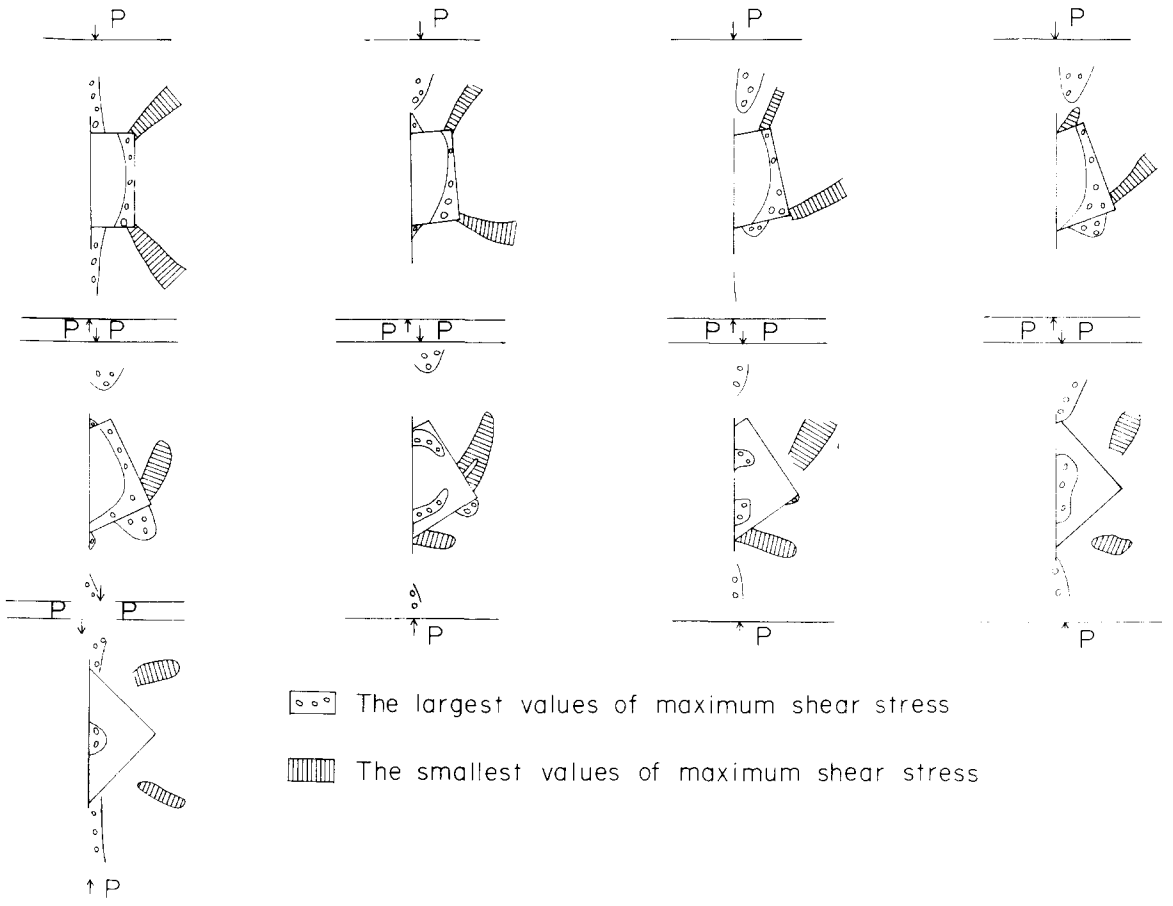

Fig. 9. The distribution of shear stress at various inclinations of the competent object in relation to the applied uni-axial compression.

Schoneveld, C. 1977. A study of some typical inclusion patterns in strongly paracrystalline rotated garnets. *Tectonophysics* **39**, 453–471.

Selkman, S. 1978. Stress and displacement analyses of boudinages by the finite-element method. *Tectonophysics* **44**, 115–139.

Stephansson, O. & Berner, H. 1971. The finite-element method in tectonic processes. *Phys. Earth. Planet. Interiors* **4**, 301–321.

Strömgård, K.-E. 1973. Stress distribution during formation boudinage and pressure shadow. *Tectonophysics* **16**, 215–248.

Wilson, E. L. 1963. Finite-element analyses of two-dimensional structures. Report No. 63-2, Structures and Materials Research, Dept. Civ. Eng. University of California, USA.

Zienkiewitz, O. C. & Cheung, Y. K. 1968. *The Finite Element Method in Structural and Continuum Mechanics*. McGraw-Hill, New York.